Journal of Biomolecular NMR, **12:** 135–144, 1998.
KLUWER/ESCOM

Comparison of ^{15}N- and ^{13}C-determined parameters of mobility in melittin

Lingyang Zhu[a,*], Franklyn G. Prendergast[b] & Marvin D. Kemple[a,**]
[a]*Department of Physics, Indiana University Purdue University Indianapolis, 402 North Blackford Street, Indianapolis, IN 46202-3273, U.S.A.*
[b]*Department of Pharmacology, Mayo Foundation, Rochester, MN 55905, U.S.A.*

Received 14 November 1997; Accepted 10 January 1998

Key words: internal dynamics, model-free approach, order parameters, peptides, relaxation

Abstract

Backbone and tryptophan side-chain mobilities in the 26-residue, cytolytic peptide melittin (MLT) were investigated by ^{15}N and ^{13}C NMR. Specifically, inverse-detected ^{15}N T_1 and steady-state NOE measurements were made at 30 and 51 MHz on MLT at 22 °C enriched with ^{15}N at six amide positions and in the Trp^{19} side chain. Both the disordered MLT monomer (1.2 mM peptide at pH 3.6 in neat water) and α-helical MLT tetramer (4.0 mM peptide at pH 5.2 in 150 mM phosphate buffer) were examined. The relaxation data were analyzed in terms of the Lipari and Szabo model-free formalism with three parameters: τ_m, the correlation time for the overall rotation; S^2, a site-specific order parameter which is a measure of the amplitude of the internal motion; and τ_e, a local, effective correlation time of the internal motion. A comparison was made of motional parameters from the ^{15}N measurements and from ^{13}C measurements on MLT, the latter having been made here and previously [Kemple et al. (1997) *Biochemistry*, **36**, 1678–1688]. τ_m and τ_e values were consistent from data on the two nuclei. In the MLT monomer, S^2 values for the backbone N-H and Cα-H vectors in the same residue were similar in value but in the tetramer the N-H order parameters were about 0.2 units larger than the Cα-H order parameters. The Trp side-chain N-H and C-H order parameters, and τ_e values were generally similar in both the monomer and tetramer. Implications of these results regarding the dynamics of MLT are examined.

Abbreviations: DSS, 2,2-dimethyl-2-silapentane-5-sulfonate, sodium salt; IUPUI, Indiana University Purdue University Indianapolis; MD, molecular dynamics; MLT, melittin; NOE, steady-state nuclear Overhauser effect.

Introduction

Heteronuclear relaxation rates measured by NMR are sensitive to subnanosecond internal motions in peptides and proteins. The reasonable expectation exists that in time it should be possible to define the relationship between these motions and biological function. Accordingly, considerable effort has been invested into making, analyzing, and then interpreting relaxation rate measurements (e.g., Clore et al. (1990), Barbato et al. (1992), Kördel et al. (1992), Stone et al. (1993), Kemple et al. (1994), Mandel et al. (1995), and references below). Usually the relaxation data are analyzed using the motional-model-independent dynamical formalism of Lipari and Szabo (1982) in terms of an overall rotational correlation time (τ_m), a generalized order parameter (S^2), and an effective internal rotational correlation time (τ_e); or, alternatively, values of the spectral density at given frequencies are extracted directly (Farrow et al. (1995), Ishima et al. (1995a), Peng and Wagner, (1995), Lefèvre et al. (1996)).

* Present address: Department of Biochemistry and Molecular Biology, The University of Chicago, Chicago, IL 60637, U.S.A. This work is in partial fulfillment of the requirements for the degree of Doctor of Philosophy in Physics. ** To whom correspondence should be addressed.

Although extensive NMR data exist on protein and peptide dynamics, questions remain regarding the accuracy of the derived motional parameters and the validity of the subsequent inferences drawn therefrom. These questions are not easily answered. One approach is to try to corroborate the NMR results by use of other spectroscopic data (Weaver et al., 1989; Palmer et al., 1993; Kemple et al., 1994,1997). Additionally, one may take advantage of NMR measurements on more than one nuclear species (Wand et al., 1996). A third approach is to compare predictions of internal motion from molecular dynamics (MD) simulations with NMR relaxation results (Chandrasekhar et al., 1992; Kördel and Teleman, 1992; Palmer and Case, 1992; Eriksson et al., 1993; Ishima et al., 1995b; Smith et al., 1995a,b; Yamasaki et al., 1995; Zheng et al., 1995; Fox and Kollman, 1996; Fushman et al., 1997). Finally, combinations of the above may be used. Smith et al. (1995b) directly compared both ^{15}N and ^{13}C T_1, T_2, and NOE values calculated from MD simulations with measurements on bovine pancreatic trypsin inhibitor, and Fadel et al. (1995) compared S^2 values calculated from MD simulations for amide N-H and Cα-H bonds in a 50-residue protein, human transforming growth factor. The latter simulations implied the existence of anticorrelated motions of adjacent backbone dihedral angles, which are called 'librational crankshaft' motions and which apparently lead to the prediction of amide N-H order parameters being smaller than Cα-H order parameters. From NMR measurements on ubiquitin, Wand and coworkers (Schneider et al., 1992; Wand et al., 1996) found N-H order parameters to be smaller than Cα-H order parameters in regions of secondary structure, with the opposite relationship prevailing elsewhere in the protein. In another case, apparently good quantitative agreement between ^{13}C (LeMaster and Kushlan, 1996) and ^{15}N (Stone et al., 1993) relaxation data on thioredoxin was found. However, LeMaster and Kushlan did not use the Lipari and Szabo approach while Stone et al. did, making a direct comparison of the motional parameters from the two studies difficult. Apart from a description of the determination of overall rotational diffusion tensors (Lee et al., 1997), to our knowledge there are no other direct comparisons of ^{15}N and ^{13}C measurements of dynamics on the same protein or peptide in the literature. This possibly is due in part to the difficulty of interpreting ^{13}C relaxation measurements in uniformly enriched proteins (Yamazaki et al., 1994), or to low NMR sensitivity in samples with ^{13}C at natural abundance, or to the cost inherent in making specific, fractional, or alternate ^{13}C-labeled proteins (LeMaster and Kushlan, 1996; Wand et al., 1996) and peptides.

In the current work we sought to answer a simple question, namely, are backbone and side-chain motional parameters determined from ^{13}C and ^{15}N relaxation measurements in peptides and folded proteins the same within reasonable error? We again choose melittin (MLT) as the model system for study largely because of its ability to exist either as a disordered, 'random-coil' monomer or a primarily α-helical, protein-like tetramer in aqueous solutions depending on conditions such as pH, and MLT and phosphate concentrations. (See Dempsey (1990) and Zhu et al. (1995) for complete references.) Moreover, we already have a substantial amount of NMR-derived dynamical data on MLT from ^{13}C NMR measurements (Kemple et al., 1997), and the molecule is easily synthesized with specific labels incorporated.

Materials and Methods

Materials

MLT, which has the sequence G-I-G-A-V-L-K-V-L-T-T-G-L-P-A-L-I-S-W-I-K-R-K-R-Q-Q, was synthesized at the Peptide Core Facility at the Mayo Foundation by solid-phase techniques as described previously (Yuan et al., 1996). To avoid the possibility of signal overlap, two selectively ^{15}N-labeled MLT preparations were made: one enriched in the amide positions of Gly^3, Leu^9 and Ala^{15}, and the other enriched in the amide positions of Gly^{12}, Leu^{16}, and Trp^{19} and in the ϵ_1 position of Trp^{19}. Since the earlier work (Kemple et al., 1997) indicated that tetramer dynamics was dependent on the presence of phosphate in the solution, an MLT sample enriched with ^{13}C at the αC position of Leu^9, and Leu^{13}, and at the δ_1 position of Trp^{19} also was synthesized to allow comparisons of tetramer dynamics at the same phosphate concentration. Isotopically enriched amino acids were purchased from Cambridge Isotope Laboratories.

Disordered (random-coil) monomeric MLT was produced by dissolving the ^{15}N-enriched peptides at a concentration of 1.2 mM in neat water at pH 3.6. Tetrameric MLT was obtained by dissolving the peptides at a concentration of 4.0 mM in an aqueous solution of 150 mM potassium phosphate buffer at pH ∼5.2. (See below for the rationale and justification of these conditions.) D_2O was added at 10% by volume to each sample for frequency locking the spectrometer.

Tetramer was formed from the ^{13}C-enriched peptide at an MLT concentration of 4.2 mM at a pH of 5.3 (not corrected) in 150 mM phosphate in D_2O. The MLT concentration was verified in each case by measuring the optical density at 280 nm and using an extinction coefficient of 5700 $M^{-1}cm^{-1}$. A capillary containing about 20 μl of 2 M $^{15}NH_4NO_3$ in 5 M HNO_3 was used as an external reference for both the ^{1}H (7.02 ppm) and ^{15}N (0 ppm) spectra. ^{13}C signals were referenced to DSS (Wishart et al., 1995).

NMR spectroscopy

^{15}N T_1 and the (steady-state) NOE of the MLT monomer and tetramer were measured at 22 $\pm$ 1 °C at two frequencies: 50.7 MHz on a Varian Unity 500 spectrometer (IUPUI) and 30.4 MHz on a Bruker AMX 300 spectrometer (Mayo Foundation) using two-dimensional, sensitivity-enhanced, proton detection (Kay et al., 1989; Stone et al., 1992). ^{13}C relaxation measurements were made on the MLT tetramer at two different frequencies using direct detection as described previously (Kemple et al., 1997). Typically, the ^{15}N T_1 and NOE spectra were recorded as 32 $\times$ 2048 (on the Varian spectrometer) or 32 $\times$ 1024 (on the Bruker spectrometer) complex matrices with 32 to 512 scans per t_1 point and with spectral widths of 1500 and 8000 Hz in the F1 (^{15}N) and F2 (^{1}H) dimensions, respectively. Recycle delays of 2–4 s for T_1 were employed. T_1 experiments on the monomer were recorded with 12 or 14 relaxation delays from 20 to 1500 ms on the Varian 500 MHz machine, and with 10 or 11 delays from 26.5 to 1203 ms on the Bruker 300 MHz machine. For the tetramer, T_1 experiments were recorded with 11 or 12 delays from 25 to 1025 ms on the Varian spectrometer, and with 10 delays from 17 to 515 ms on the Bruker spectrometer. ^{15}N NOE values were determined from spectra, recorded with and without ^{1}H saturation, and with recycle delays of 3–5 s.

Particular attention was paid to certain aspects of the ^{15}N experiments. The influence of proton exchange on the ^{15}N NOE values was minimized by using long (>8 T_1 for most residues) recycle delays between each acquisition (Grzesiek and Bax, 1993). ^{1}H saturation during the relaxation delay in T_1 experiments was accomplished by a ^{1}H GARP sequence (Shaka et al., 1985) or a series of ^{1}H π-pulses with a 2 ms separation. ^{1}H saturation in the NOE experiments was achieved by ^{1}H GARP pulses with 3 s and 2 s irradiation periods for the monomer and tetramer, respectively. Low-power presaturation of the water signal for 100 ms in NOE experiments and a spin-lock purge pulse with a locking period in the range 0.8–2 ms in both T_1 and NOE experiments were used to suppress the water signal. ^{15}N decoupling during the acquisition periods in T_1 and NOE experiments was achieved by Waltz-16 pulse sequences (Shaka et al., 1983) at an $\sim$1 kHz field strength.

Vnmr 4.3 (Varian) and Felix 95 (Biosym Inc.) were used for data processing. The data were zero-filled (Vnmr) or extended by linear prediction (Felix), multiplied by weighting functions (Gaussian or a squared, shifted sine-bell), and then transformed to give the final matrices of 256 (F1) $\times$ 2048 (F2) points. Polynomial baseline corrections were applied to the processed spectra in F2. A polynomial function of up to seven orders was also used to filter the water signal when NOE data were processed using Felix 95. The intensities of cross peaks in the two-dimensional spectra were characterized from peak heights (for NOE) or volumes (for T_1). T_1 values were extracted from nonlinear least-squares fits of a single exponential, three-parameter function of the form $I(t) = I_\infty - (I_\infty - I_0)\exp(-t/T_1)$ to the measured cross-peak intensities of the two-dimensional spectra collected with different relaxation delays, t. Figure 1 shows typical relaxation curves from tetrameric MLT at 50.7 MHz. The uncertainties in T_1 were generated, in most cases, during the fitting process by giving deviations of $\pm$5% in intensity to each point. These derived uncertainties were consistent with differences in repeated measurements. NOE was calculated as the ratio of the peak intensities with and without proton saturation. The mean NOE values and their standard deviations were determined from 2–3 independent measurements. The deviations were found generally to be less than 10%. When only one NOE experiment was performed, the standard deviation in the NOE, σ_{NOE}, was calculated on the basis of measured background noise levels using the relationship $\sigma_{NOE}/NOE = ((\sigma_{SAT}/I_{SAT})^2 + (\sigma_{UNSAT}/I_{UNSAT})^2)^{1/2}$ (Torchia et al., 1993).

To be able to do ^{15}N relaxation measurements with inverse detection, the pH needs to be relatively low because of proton exchange, but the MLT tetramer is less stable at acidic conditions. To solve this problem, we first established conditions for the tetramer by pH titrations of selectively ^{13}Cα-labeled MLT in 150 mM phosphate buffer at different MLT concentrations (1–4 mM). By making use of the dependence of ^{13}Cα chemical shifts on MLT conformation, the observation that monomer and tetramer are in slow exchange when

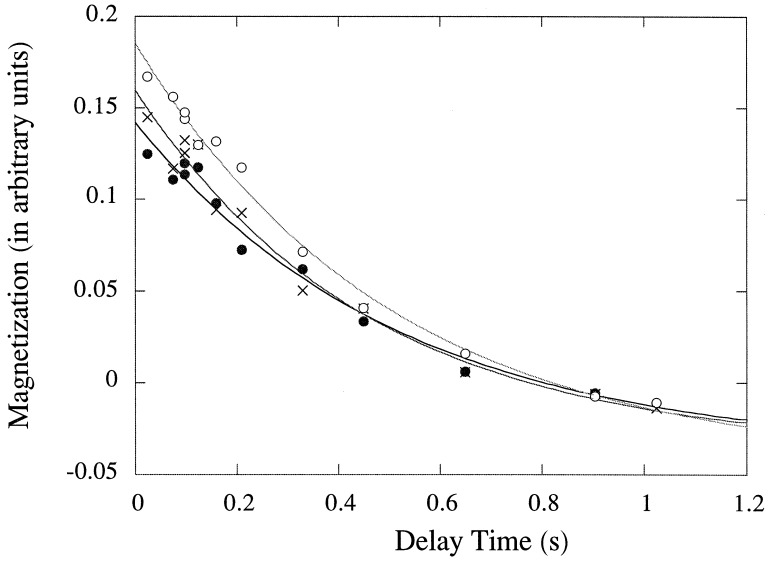

Figure 1. ^{15}N T_1 recovery curves of tetrameric MLT at a ^{15}N resonance frequency of 50.7 MHz. Data points for the amide ^{15}N of Gly^3, Leu^9, and Ala^{15} are represented by o, x, and •, respectively.

Table 1. Chemical shifts of ^{1}H and ^{15}N of melittin[a]

Label[b]	δ (^{1}H) (ppm)		δ (^{15}N) (ppm)	
	Monomer	Tetramer	Monomer	Tetramer
G3am	8.45	8.76	92.16	90.25
L9am	8.16	8.06	102.63	97.55
G12am	8.28	8.28	89.99	89.75
A15am	8.35	7.27	105.82	98.55
L16am	8.00	8.04	102.75	102.25
W19am	8.00	8.04	100.46	100.37
W19ϵ_1	10.07	10.51	108.75	109.84

[a] A capillary containing 2 M $^{15}NH_4NO_3$ in 5 M HNO_3 served as external reference for both ^{1}H (7.02 ppm) and ^{15}N (0 ppm). Chemical shift values were reproducible to ±0.03 ppm.

[b] The abbreviation 'am' is used to designate the amide nitrogen.

signals are present from both species, and available ^{13}C NMR spectra of MLT (Buckley et al., 1993; Zhu et al., 1995), we found that at concentrations above 3 mM, MLT in 150 mM phosphate buffer is predominantly tetrameric at pH values of ∼4. These results led to the choice of sample conditions given above. The phosphate concentration is higher than that used in the previous study (50 mM; Kemple et al. (1997)).

Results and Discussion

The ^{1}H and ^{15}N assignments of the ^{15}N-enriched residues in the monomer and tetramer were made from COSY, TOCSY, and HMQC experiments with reference to the work of Brown et al. (1980), Lauterwein et al. (1980), and Buckley et al. (1993), and the ^{1}H and ^{15}N chemical shifts are listed in Table 1. The chemical shift differences between monomer and tetramer are residue and nucleus dependent and are consistent with the presence of helical structure in the tetramer (Wishart et al., 1991). Similar changes were found earlier for amide proton (Buckley et al., 1993) and ^{13}Cα chemical shifts in MLT (Buckley et al., 1993; Zhu et al., 1995; Yuan et al., 1996; Kemple et al., 1997).

The ^{15}N relaxation data are given in Table 2. Since ^{15}N has a negative gyromagnetic ratio, the ^{15}N-^{1}H steady-state NOE can be negative or positive depending on the specifics of the motion. Larger NOE values generally imply a larger overall rotational correlation time and/or more restricted motion. Both of these trends are apparent in Table 2 in the larger NOE values of the tetramer. (See the results of the analysis below.)

The ^{13}C relaxation data for the disordered monomer from Kemple et al. (1997) are given in Table 3 for completeness, and the ^{13}C chemical shift and relaxation data for the tetramer formed at sample conditions similar to those used in the ^{15}N measurements (see the Materials and Methods section) are summarized in Table 4. The chemical shifts of the

Table 2. ^{15}N T_1 and NOE of melittin in aqueous solution

Label	30.4 MHz		50.7 MHz	
	T_1(s)	NOE	T_1(s)	NOE
Monomer				
G3am	0.81 ± 0.12	-2.30 ± 0.34	1.32 ± 0.19	-1.50 ± 0.20
L9am	0.52 ± 0.05	-2.00 ± 0.20	0.60 ± 0.06	
G12am	0.48 ± 0.08	-1.23 ± 0.18	0.92 ± 0.09	-0.74 ± 0.11
A15am	0.49 ± 0.04	-1.48 ± 0.14	0.71 ± 0.07	-0.47 ± 0.07
L16am	0.42 ± 0.04	-0.95 ± 0.09	0.58 ± 0.05	-0.30 ± 0.03
W19am	0.56 ± 0.07	-0.84 ± 0.15	0.62 ± 0.09	-0.40 ± 0.06
W19ϵ_1	0.48 ± 0.04	-1.37 ± 0.21	0.85 ± 0.12	-0.81 ± 0.12
Tetramer				
G3am	0.28 ± 0.04	0.33 ± 0.05	0.50 ± 0.07	0.74 ± 0.11
L9am	0.28 ± 0.01	0.55 ± 0.05	0.46 ± 0.04	0.67 ± 0.06
G12am	0.31 ± 0.03	0.41 ± 0.04	0.48 ± 0.03	0.69 ± 0.06
A15am	0.33 ± 0.03	0.55 ± 0.05	0.32 ± 0.03	0.72 ± 0.07
L16am	0.31 ± 0.01	0.46 ± 0.03	0.52 ± 0.02	0.70 ± 0.07
W19am	0.31 ± 0.01	0.46 ± 0.03	0.45 ± 0.01	0.60 ± 0.06
W19ϵ_1	0.36 ± 0.03	0.53 ± 0.05		0.51 ± 0.07

two backbone residues examined in the tetramer under these conditions (Leu^9 and Leu^{13}) agree with the previously published values for the tetramer formed at lower phosphate concentration and higher pH (Kemple et al., 1997).

Analysis of the relaxation data

The relaxation of the ^{15}N or ^{13}C magnetization is caused by modulation, due to the rotational motion of the molecule, of the ^{15}N- or ^{13}C-proton dipolar interaction and of the chemical shift anisotropy. The relevant T_1 and NOE formulas used here are given in Kemple et al. (1997) for ^{13}C and were adapted to ^{15}N by interchanging the ^{13}C gyromagnetic ratio with that of ^{15}N. The motion enters the problem through the spectral density $J(\omega)$, where ω is the angular frequency. Accordingly, the form that is used for $J(\omega)$ is central to the data interpretation. Here we used the motional-model-free approach of Lipari and Szabo (1982) in which

$$J(\omega) = \frac{2}{5}\left[\frac{S^2\tau_m}{1+\omega^2\tau_m^2} + \frac{(1-S^2)\tau}{1+\omega^2\tau^2}\right]$$

where τ_m is the correlation time of the overall rotation of the molecule, and S^2 is the generalized order parameter and τ_e is the effective correlation time for the internal motion of the N-H or C-H vector within the molecule where $\tau^{-1} = \tau_m^{-1} + \tau_e^{-1}$. The overall rotational motion was taken to be isotropic as was shown earlier to be appropriate for monomeric and tetrameric MLT (Kemple et al., 1997). The motional parameters τ_m, τ_e, and S^2 were found by least-squares fitting the relaxation data to the applicable equations using the program Modelfree 3.1 written by Art Palmer of Columbia University. The fitting procedure, which is described in Kemple et al. (1997), follows the prescription of Mandel et al. (1995). The overall quality of the fits was assessed from

$$\chi^2 = (N - N_P)^{-1} \sum_{i=1}^{N} (m_i - c_i)^2/\sigma_i^2$$

where N is the total number of data, N_P is the total number of parameters, m_i and c_i are the measured and calculated values of T_1 and NOE, and σ_i are the estimated uncertainties in the measured values, and by fits of data sets generated from Monte Carlo simulations (500 in each case). The quoted uncertainties in the parameters were derived from the fits of the simulated data given by Modelfree 3.1. In no case was an additional order parameter (Clore et al., 1990) required to fit the data within 95% confidence limits.

For monomeric MLT, two approaches were followed in extracting the motional parameters. In one, the ^{15}N relaxation data alone were fit, and in the second the ^{15}N data were combined with the ^{13}C relaxation data to obtain a common basis for comparison. (We ignored the potential consequences of

Table 3. ^{13}C T_1 and NOE of disordered melittin monomer[a]

Label	75.4 MHz		125 MHz	
	T_1(s)	NOE	T_1(s)	NOE
G1α	0.28	2.13	0.39	2.07
G3α	0.16	2.24	0.22	2.15
A4α	0.25	1.98	0.39	1.82
L6α	0.19	1.87	0.30	1.77
L9α	0.19	1.83	0.30	1.72
G12α	0.13	1.67	0.20	1.57
L13α	0.20	1.76	0.29	1.61
A15α	0.20	1.69	0.32	1.61
L16α	0.19	1.59	0.32	1.45
W19δ_1	0.19	1.61	0.26	1.50
W19ϵ_3	0.17	1.44	0.25	1.41

[a] Data from Kemple et al. (1997). Uncertainties in T_1 and NOE were ±5%.

the 2 °C temperature difference in the two sets of experiments.) The derived motional parameters agreed within the experimental uncertainties whether or not the ^{15}N and ^{13}C data were analyzed together. Accordingly, in Table 5 we list the motional parameters obtained for the monomer from the combined fitting. The τ_m value, 1.5 ± 0.1 ns, conforms with that given in Kemple et al. (1997) (1.3 ± 0.1 ns). There are differences between the ^{13}C S^2 and τ_e values given here and in Kemple et al. (1997) because the τ_m values are not identical, but these differences are insignificant. The monomer data also were fitted by assigning individual τ_m values to the labeled positions as was done in Kemple et al. (1997) and these values matched the global τ_m within the errors.

It can be seen from Table 5 that the ^{15}N and ^{13}C order parameters for corresponding backbone positions in monomeric disordered MLT are identical within the uncertainties. The τ_e values found for the backbone N-H vectors agree reasonably with those found for the Cα-H vectors and are in the motional narrowing limit. The Trp side-chain order parameters also agree well for the two nuclei, but the τ_e value for the (^{15}N) ϵ_1 position is larger than τ_e for the (^{13}C) ϵ_3 and δ_1 positions. Note that the N-H order parameter for Gly^3 is in keeping with 'end effects' (cf. Kemple et al. (1997)). The amide N-H order parameter for Gly^{12} is smaller than those of the other 'interior' positions consistent with the Cα-H order parameters (Kemple et al., 1997). Overall, both amide N-H and Cα-H (Kemple et al., 1997) order parameters are larger in the second half of the MLT sequence than in the first half. Thus, as observed in the earlier work, the order parameter differences across the structure presumably reflect end effects and the existence of transient secondary structure in the disordered monomer.

The ^{15}N and ^{13}C data of the tetramer given in Tables 2 and 4 were combined to yield the motional parameters shown in Table 6. Also included in Table 6 to facilitate comparisons are motional parameters obtained for the tetramer generated in 50 mM phosphate at pH 9 (Kemple et al., 1997). The τ_m of 4.3 ± 0.2 ns obtained here is the same within the uncertainties as τ_m found by Kemple et al. (1997) (4.2 ± 0.5 ns) for the tetramer in phosphate, and the ^{13}C S^2 values and τ_e values are consistent from the two studies despite the relatively large errors inherent in τ_e determinations. Again corroborating the result of Kemple et al. (1997), the order parameter of the N-H vector of Gly^3 is not smaller in the tetramer relative to the interior positions in contrast to the results obtained for the disordered monomer. The decreased mobility of Gly^3 in the tetramer almost certainly derives from the stabilization of the helical form due to interhelical interactions. Comparison of backbone nitrogen order parameters and backbone Cα order parameters in Table 6 for the tetramer on a residue-by-residue basis reveals that the N-H order parameters are consistently larger by ∼0.2 of a unit. In particular, the average of the backbone N-H order parameters is 0.70 ± 0.04 and the average of the Cα-H S^2 values is 0.50 ± 0.04. On the other hand, the W19ϵ_1-H order parameter is similar in value to the Trp side-chain order parameter values found from the ^{13}C measurements. Although the Gly^{12} Cα-H S^2 in the tetramer was smaller than that for other interior backbone positions (Kemple et al., 1997), such was not the case for the Gly^{12} amide N-H order parameter. This may be a direct reflection of H-bonding.

The amide N-H S^2 values are larger in the tetramer than in the monomer as is apparent in Tables 5 and 6 and Figure 2 as we would expect, a priori. However, this tendency is not present in the Cα order parameters for the tetramer in 50 mM phosphate at pH 9 (Kemple et al., 1997) or here for the tetramer in 150 mM phosphate at pH 5.2. The disparity in behavior of the ^{15}N- and ^{13}C-derived motions is not readily explained but may be a result of hydrogen bonding between amide nitrogen atoms and carbonyls in the tetramer. There are also differences between the backbone N-H τ_e values for the monomer and tetramer τ_e being consistently larger in the monomer. This effect was observed earlier by Kemple et al. (1997) in ^{13}C

Table 4. ^{13}C chemical shifts[a], T_1, and NOE for tetrameric melittin

Label	δ (ppm)	75.4 MHz		125.7 MHz	
		T_1 (s)	NOE	T_1 (s)	NOE
L9α	57.36	0.30 ± 0.02	1.27 ± 0.04	0.69 ± 0.03	1.36 ± 0.06
L13α	59.00	0.27 ± 0.02	1.28 ± 0.02	0.63 ± 0.04	1.25 ± 0.06
W19δ_1	127.60	0.24 ± 0.01	1.32 ± 0.04	0.47 ± 0.02	1.24 ± 0.10

[a]Referenced to DSS at 0 ppm.

Table 5. Motional parameters for monomeric melittin[a]

Label	^{15}N labels		^{13}C labels	
	S^2	τ_e (ps)	S^2	τ_e (ps)
G1	–	–	0.13 ± 0.01	39 ± 4
G3	0.18 ± 0.02	100 ± 18	0.19 ± 0.02	92 ± 8
A4	–	–	0.34 ± 0.03	83 ± 11
L6	–	–	0.45 ± 0.03	134 ± 22
L9	0.39 ± 0.05	179 ± 28	0.46 ± 0.03	119 ± 20
G12	0.34 ± 0.03	81 ± 17	0.39 ± 0.02	45 ± 8
L13	–	–	0.50 ± 0.03	104 ± 18
A15	0.48 ± 0.04	120 ± 25	0.50 ± 0.03	76 ± 14
L16	0.61 ± 0.05	141 ± 46	0.56 ± 0.03	49 ± 15
W19	0.51 ± 0.05	97 ± 26	–	–
W19δ_1	–	–	0.51 ± 0.03	75 ± 16
W19ϵ_1	0.47 ± 0.04	142 ± 34	–	–
W19ϵ_3	–	–	0.55 ± 0.03	49 ± 15

[a] $\tau_m = 1.5 \pm 0.1$ ns, $\chi^2 = 1.48$. Unless otherwise designated in the first column, the ^{15}N labels are at the amide position and the ^{13}C labels are at the α position. The numerical values used in the analysis were: proton-nitrogen distance, 1.02 Å; proton-carbon distance, 1.09 Å; amide ^{15}N CSA, $\delta_{zz} = -(\frac{2}{3})$ (160 ppm), $\eta = 0$, Hiyama et al. (1988); ^{15}N Trp ϵ_1 CSA, $\delta_{zz} = 59$ ppm, $\eta = 0.66$, Cross and Opella (1983); for ^{13}C CSA parameters, see Yuan et al. (1996).

measurements. We infer that tighter packing of the residues in the tetramer results in damping of the rate of internal motion.

It is worth noting that due to the strong dependence of the relaxation rates on bond distance, a relatively small variation in that distance can lead to a much larger change in order parameter. In particular, a change in bond distance of only ∼6% could account for the differences observed between the ^{15}N and ^{13}C backbone order parameters in the tetramer. On the other hand, if there were such a change in the C-H or N-H distance or a combination of both in the sense to bring the tetramer order parameters into consonance, the monomer order parameters would then disagree. Any systematic changes of the C-H or N-H distances, however, would not affect the relative differences (or lack thereof) observed for a given nucleus between the monomer and tetramer. This aside, we continue our discussion based upon the results presented in Tables 5 and 6.

What do these data say regarding the physical model of peptide dynamics? In the case of monomeric, disordered MLT, since the backbone N-H order parameters were similar to the Cα-H order parameters, estimates of the angular amplitudes of the motion given in the previous paper (Kemple et al., 1997) for a restricted diffusion model (London and Avitabile, 1978) seem reasonable. But there are alternative explanations. For example, MD simulations of ribonuclease H1 (Yamasaki et al., 1995) predicted that the region of space sampled by amide N-H vectors in that protein could be approximated as a cone with an elliptical cross section, and similar observations were made by Zheng et al. (1995) and Fushman et al. (1997) for other proteins. These motions are similar to the Kinosita model (Kinosita et al., 1977) where the cross section of the cone is circular. Assuming that the model could apply to a disordered system (the monomer) and the folded protein-like environment of the tetramer, we note that there are not enough measured motional parameters to justify attempting to find the dimensions of cones with elliptical cross sections, but it is straightforward to calculate the half-angle, α, of the cone in the Kinosita model ($S^2 = \frac{1}{4}\cos^2\alpha(1+\cos\alpha)^2$). The average backbone N-H order parameters from the monomer (0.39 excluding Gly^3) and the tetramer (0.70) give $\alpha = 44°$ and 27°, respectively.

Our previous results on monomeric, helical MLT (in methanol) (Kemple et al., 1997) yielded angular motions broadly consistent with crankshaft motions present in MD simulations of an α-helical peptide (Daggett et al., 1991). As noted above, MD simulations on a small protein (Fadel et al., 1995), which also suggested crankshaft-like motions, predicted that N-H order parameters should be smaller than Cα-

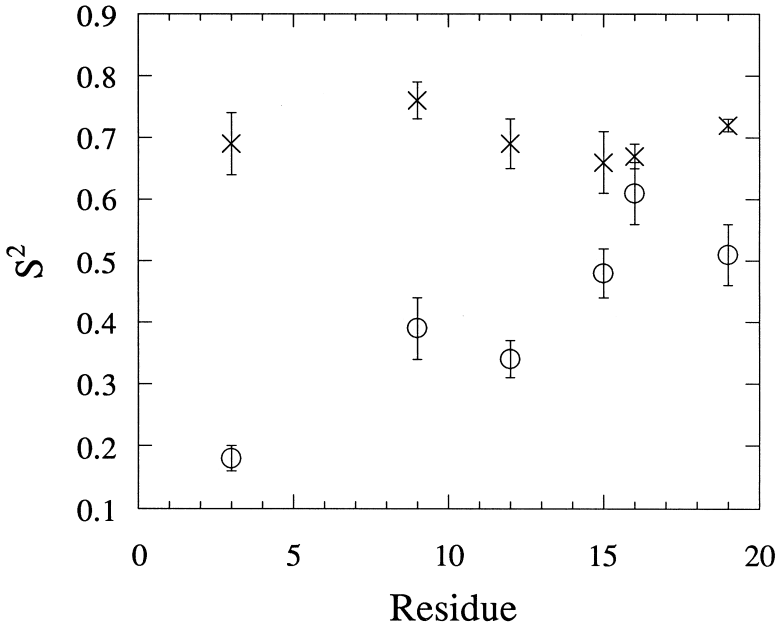

Figure 2. Backbone ^{15}N-H order parameters for monomeric (○) and tetrameric (X) melittin displayed by sequence number.

Table 6. Motional parameters for tetrameric melittin[a]

Label	^{15}N labels		^{13}C labels[b]		^{13}C labels[c]	
	S^2	τ_e (ps)	S^2	τ_e (ps)	S^2	τ_e (ps)
G3	0.69 ± 0.05	47 ± 24	–	–	0.48 ± 0.03	10 ± 4
L9	0.76 ± 0.03	14 ± 14	0.52 ± 0.03	15 ± 4	–	–
G12	0.69 ± 0.04	33 ± 16	–	–	0.42 ± 0.02	7 ± 3
L13	–	–	0.58 ± 0.03	11 ± 5	0.52 ± 0.03	7 ± 7
A15	0.66 ± 0.05	5 ± 5	–	–	0.51 ± 0.02	8 ± 4
L16	0.67 ± 0.02	20 ± 12	–	–	0.47 ± 0.02	2 ± 2
W19	0.72 ± 0.01	38 ± 14	–	–	–	–
W19δ_1	–	–	0.60 ± 0.04	30 ± 11	0.52 ± 0.04	21 ± 10
W19ϵ_1	0.62 ± 0.06	17 ± 12	–	–	–	–
W19ϵ_3	–	–	–	–	0.54 ± 0.05	14 ± 11

[a] $\tau_m = 4.3 \pm 0.2$ ns, $\chi^2 = 1.21$ based on fitting the data in Tables 2 (4.0 mM peptide in 150 mM phosphate at pH 5.2) and 4 (4.2 mM peptide in 150 mM phosphate at pH 5.3). Unless otherwise designated in the first column, the ^{15}N labels are at the amide position and the ^{13}C labels are at the α position. The nuclear distances and the CSA parameters are given in Table 5.

[b] From the data in Table 4.

[c] From Kemple et al. (1997) (1 mM peptide in 50 mM phosphate at pH 9).

H order parameters. However, for the MLT tetramer which approximates a folded protein of mass ~11 000, our experimental results are just the opposite of the predictions of the MD simulations. In general where comparisons from MD simulations on other systems exist in the literature, backbone N-H order parameters tend to be smaller than Cα-H S^2 values (Palmer and Case, 1992; Smith et al., 1995b; also see Fadel et al. (1995)). Wand et al. (1996) did find Cα-H order parameters to be larger than amide order parameters in the backbone of ubiquitin where there was a definite secondary structure although the measured amide order parameters are smaller than values calculated from MD simulations (Fox and Kollman, 1996). They also

derived τ_e values from ^{13}C measurements in ubiquitin that were larger than those from ^{15}N measurements. In our case for both the MLT monomer and tetramer, if anything, the amide τ_e values were slightly larger.

Given this information, we are left with the speculation that the difference between our results on the MLT tetramer and those of the simulations (on other systems) may derive from the effects of H-bonding. Taking H-bonding into account in MD simulations is difficult and the extent to which calculated order parameters are affected by H-bonding is unclear at this point. MD simulations of rat intestinal fatty acid binding protein (V. Likic and F.G. Prendergast, unpublished results) show a correlation of order parameter values with secondary structure, but no appreciable correlation of order parameters with the number of H-bonds. In particular, the average values of amide bond order parameters increase in going from β-ribbon to α-helical regions, with Cα-H order parameters following a less pronounced, but opposite, pattern. However, the former still remain smaller on average than the latter. The MLT tetramer, as noted, is primarily α-helical so, generally speaking, the increase in amide-N order parameters relative to the Cα-H order parameters in the tetramer is consistent with the predictions of these simulations. On the other hand, the applicability of protein simulations to the tetramer is questionable; the tetramer is not a globular protein, its four strands being held together by hydrophobic forces. Clearly, more work is required to resolve these issues. The larger backbone N-H order parameters observed here in the tetramer relative to the Cα-H order parameters are at least consistent with the participation of the amide nitrogen in the peptide bond, the latter having a partial double bond character.

Lastly, it is worthwhile to consider models of the Trp side-chain dynamics inferred from these data. A number of simple models for the motion of the Trp side chain were discussed in Kemple et al. (1997). The addition of an order parameter for a third vector ($N\epsilon_1$-H) in the indole ring, not parallel to the original two vectors ($C\delta_1$-H and $C\epsilon_3$-H), places further constraints on the models. The previous conclusion of the inappropriateness of a model of restricted diffusion about the β-γ bond in the disordered monomer and the tetramer holds. On the other hand, models describing jumps of the indole ring between two orientations about the β-γ bond do not work for either state of MLT regardless of the angular size of the jumps or the relative populations of the sites, even though the ^{13}C data alone were consistent with such a motion for the monomer (Kemple et al., 1997). Taking all three order parameters into account clearly rules out the two-site jump model. When motion of the trp ring about the α-β bond alone is considered for the tetramer, a three-site jump model with equal-angle jumps in which

$$S^2 = \frac{1}{4}(3\ \cos^2\ \theta - 1)^2 + \frac{3}{4}(\sin^2\ 2\theta + \sin^4\ \theta)\times (p_1^2 + p_2^2 + p_3^2 - p_1p_2 - p_2p_3 - p_3p_1)$$

(where θ is the angle between the given C-H vector and the α-β bond and where the relative fractional populations of the sites p_1, p_2, and p_3 are ∼0.8, 0.1, and 0.1) gives good agreement with all three measured order parameters. (This model was not applied to the monomer because the angles that the $N\epsilon_1$-H, $C\delta_1$-H, and $C\epsilon_3$-H vectors make with the α-β bond are not known.) From these results, it is apparent that the actual motion of the indole moiety cannot be a simple rotation, and that it is not easy to construct a physical description of the motion, a reality which reinforces the utility of the Lipari and Szabo approach.

Conclusions

In summary, the essentially identical values of τ_m obtained from measurements on the two different nuclei affirm the robustness of its determination by the use of T_1 and NOE values. The identity of the ^{13}C- and ^{15}N-derived backbone order parameters in the interior of the disordered peptide is physically sensible. Also, both the ^{13}C and ^{15}N measurements showed the presence of end effects at Gly^3 in the monomer and their subsequent disappearance in the more structurally stabilized environment of the tetramer. The amide S^2 values are larger in the tetramer as expected, but the disparity between the order parameters for the $^{13}C\alpha$ and the amide ^{15}N-H vectors is an unexpected and as yet unexplained result which does not bear out inferences made from MD simulations (Fadel et al., 1995). Moreover, while these data are insufficient to refute a so-called crankshaft model for motion about the peptide bond in tetrameric MLT, they do run counter to the physical predictions of such a model.

Acknowledgements

We thank Drs. Slobodan Macura and Nenad Juranic at Mayo, and Durgu Rao and Bruce Ray at the IUPUI NMR Center for advice and technical assistance. This

work was supported in part by NSF Grant DMB-9105885 to M.D.K. and by PHS Grant GM34847 to F.G.P.

References

Barbato, G., Ikura, M., Kay, L.E., Pastor, R.W. and Bax, A. (1992) *Biochemistry*, **31**, 5269–5278.

Brown, L.R, Lauterwein, J. and Wüthrich, K. (1980) *Biochim. Biophys. Acta*, **622**, 231–244.

Buckley, P., Edison, A.S., Kemple, M.D. and Prendergast, F.G. (1993) *J. Biomol. NMR*, **3**, 639–652.

Chandrasekhar, I., Clore, G.M., Szabo, A., Gronenborn, A.M. and Brooks, B.R. (1992) *J. Mol. Biol.*, **226**, 239–250.

Clore, G.M., Szabo, A., Bax, A., Kay, L.E., Driscoll, P.C. and Gronenborn, A.M. (1990) *J. Am. Chem. Soc.*, **112**, 4989–4991.

Cross, T.A. and Opella, S.J. (1983) *J. Am. Chem. Soc.*, **105**, 306–308.

Daggett, V., Kollman, P.A. and Kuntz, I.D. (1991) *Biopolymers*, **31**, 1115–1134.

Dempsey, C.E. (1990) *Biochim. Biophys. Acta*, **1031**, 143–161.

Eriksson, M.A.L., Berglund, H., Härd, T. and Nilsson, L. (1993) *Proteins Struct. Funct. Genet.*, **17**, 375–390.

Fadel, A.R., Jin, D.Q., Montelione, G.T. and Levy, R.M. (1995) *J. Biomol. NMR*, **6**, 221–226.

Farrow, N.A., Zhang, O., Szabo, A., Torchia, D.A. and Kay, L.E. (1995) *J. Biomol. NMR*, **6**, 153–162.

Fox, T. and Kollman, P.A. (1996) *Proteins Struct. Funct. Genet.*, **25**, 315–334.

Fushman, D., Cahill, S. and Cowburn, D. (1997) *J. Mol. Biol.*, **266**, 173–194.

Grzesiek, R. and Bax, A. (1993) *J. Am. Chem. Soc.*, **115**, 12593–12594.

Hiyama, Y., Niu, C., Silverton, J.V., Bavoso, A. and Torchia, D.A. (1988) *J. Am. Chem. Soc.*, **110**, 2378–2383.

Ishima, R., Yamasaki, K. and Nagayama, K. (1995a) *J. Biomol. NMR*, **6**, 423–426.

Ishima, R., Yamasaki, K., Saito, M. and Nagayama, K. (1995b) *J. Biomol. NMR*, **6**, 217–220.

Kay, L.E., Torchia, D.A. and Bax, A. (1989) *Biochemistry*, **28**, 8972–8979.

Kemple, M.D., Yuan, P., Nollet, K.E., Fuchs, J.A., Silva, N. and Prendergast, F.G. (1994) *Biophys. J.*, **66**, 2111–2126.

Kemple, M.D., Buckley, P., Yuan, P. and Prendergast, F.G. (1997) *Biochemistry*, **36**, 1678–1688.

Kinosita, K.S., Kawato, S. and Ikegami, A. (1977) *Biophys. J.*, **20**, 289–305.

Kördel, J., Skelton, N.J., Akke, M., Palmer, A.G. and Chazin, W.J. (1992) *Biochemistry*, **31**, 4856–4866.

Kördel, J. and Teleman, O. (1992) *J. Am. Chem. Soc.*, **114**, 4934–4936.

Lauterwein, J., Brown, L.R. and Wüthrich, K. (1980) *Biochim. Biophys. Acta*, **622**, 219–230.

Lee, L.K., Rance, M., Chazin, W.J. and Palmer, A.G. (1997) *J. Biomol. NMR*, **9**, 287–298.

Lefèvre, J.-F., Dayie, K.T., Peng, J.W. and Wagner, G. (1996) *Biochemistry*, **35**, 2674–2686.

LeMaster, D.M. and Kushlan, D.M. (1996) *J. Am. Chem. Soc.*, **118**, 9255–9264.

Lipari, G. and Szabo, A. (1982) *J. Am. Chem. Soc.*, **104**, 4546–4559.

London, R.E. and Avitabile, J. (1978) *J. Am. Chem. Soc.*, **100**, 7159–7165.

Mandel, A.M., Akke, M. and Palmer, A.G. (1995) *J. Mol. Biol.*, **246**, 144–163.

Palmer, A.G. and Case, D.A. (1992) *J. Am. Chem. Soc.*, **114**, 9059–9067.

Palmer, A.G., Hochstrasser, R.A., Millar, D.P., Rance, M. and Wright, P.E. (1993) *J. Am. Chem. Soc.*, **115**, 6333–6345.

Peng, J.W. and Wagner, G. (1995) *Biochemistry*, **34**, 16733–16752.

Schneider, D.M., Dellow, M.J. and Wand, A.J. (1992) *Biochemistry*, **31**, 3645–3652.

Shaka, A.J., Keeler, J., Frenkiel, T. and Freeman, R. (1983) *J. Magn. Reson.*, **52**, 335–338.

Shaka, A.J., Barker, P.B. and Freeman, R. (1985) *J. Magn. Reson.*, **64**, 547–552.

Smith, L.J., Mark, A.E., Dobson, C.M. and van Gunsteren, W.F. (1995a) *Biochemistry*, **34**, 10918–10931.

Smith, P.E., Schaik, R.C., Szyperski, T., Wüthrich, K. and van Gunsteren, W.F. (1995b) *J. Mol. Biol.*, **246**, 356–365.

Stone, M.J., Fairbrother, W.J., Palmer, A.G., Reizer, J., Saier, M.H. and Wright, P.E. (1992) *Biochemistry*, **31**, 4394–4406.

Stone, M.J., Chandrasekhar, K., Holmgren, A., Wright, P.E. and Dyson, H.J. (1993) *Biochemistry*, **32**, 426–435.

Terwilliger, T.C. and Eisenberg, D. (1982a) *J. Biol. Chem.*, **257**, 6010–6015.

Terwilliger, T.C. and Eisenberg, D. (1982b) *J. Biol. Chem.*, **257**, 6016–6022.

Torchia, D.A., Nicholson, L.K., Cole, H.B.R. and Kay, L.E. (1993) In *NMR of Proteins* (Eds., Clore, G.M. and Gronenborn, A.M.), CRC Press, Boca Raton, FL, pp. 190–219.

Wand, A.J., Urbauer, J.L., McEvoy, R.P. and Bieber, R.J. (1996) *Biochemistry*, **35**, 6116–6125.

Weaver, A.J., Kemple, M.D. and Prendergast, F.G. (1989) *Biochemistry*, **28**, 8624–8639.

Wishart, D.S., Sykes, B.D. and Richards, F.M. (1991) *J. Mol. Biol.*, **222**, 311–333.

Wishart, D.S., Bigam, C.G., Yao, J., Abildgaard, F., Dyson, H.J., Oldfield, E., Markley, J.L. and Sykes, B.D. (1995) *J. Biomol. NMR*, **6**, 135–140.

Yamasaki, K., Saito, M., Oobatake, M. and Kanaya, S. (1995) *Biochemistry*, **34**, 6587–6601.

Yamazaki, T., Muhandiram, R. and Kay, L.E. (1994) *J. Am. Chem. Soc.*, **116**, 8266–8278.

Yuan, P., Fisher, P.J., Prendergast, F.G. and Kemple, M.D. (1996) *Biophys. J.*, **70**, 2223–2238.

Zheng, Z., Czaplicki, J. and Jardetzky, O. (1995) *Biochemistry*, **34**, 5212–5223.

Zhu, L., Kemple, M.D., Yuan, P. and Prendergast, F.G. (1995) *Biochemistry*, **34**, 13196–13202.